Simulation of H Lyman-α images for the METIS coronagraph

Bemporad A.

Rapporto nr.132 03/06/2010

Simulation of H Lyman-α images for the METIS coronagraph

A. Bemporad
INAF-Osservatorio Astronomico di Torino, via Osservatorio 20,
10025 Pino Torinese (TO), Italy; bemporad @oato.inaf.it

ABSTRACT

This report describes step by step how the images of H Lyman-α 1216Å intensity (phot cm^{-2} s^{-1} sr^{-1}) expected on the CCD detector have been constructed. In summary, the images are built starting from images of white light corona acquired by the SOHO/LASCO C2 & C3 and Mauna Loa/Mark IV coronagraphs and from Lyman-α intensities and line profiles measured by SOHO/UVCS instrument at different heliocentric distances and latitudes. A routine has been written (in IDL language) able to provide a Lyman-α image for any heliocentric distance of the Solar Orbiter spacecraft and both for the minimum and maximum phases of the solar cycle. Simulated images have then been used to estimate the expected counts number and the exposure times required to have a provided signal to noise ratio. It turns out that at solar minimum very long exposure times (up to more than ~ 3000s) will be required over the polar regions in order to have a S/N ratio of 10, while exposure times of ~ 30s will be sufficient for the equatorial regions. These exposure times have to multiplied by a factor ~2 in order to have the same S/N ratio at the line peak in the Ly-α line profile.

1. SUMMARY OF INPUT INSTRUMENTAL PARAMETERS

The METIS simulated images described here have been obtained by assuming a series of instrumental parameters, which are listed for the Reader convenience in Table 1. All these parameters can be also found in Tables 3.1, 3.3 and 4.4 of the METIS Instrument Experiment Interface Document-B (EID-B, issue 2, rel.2, 03/02/2010), except for the EUV pass-band filter width, which has been assumed to be 80 Å for the Lyman-α channel (as suggested by…). These parameters have been used to build the coronagraphic images and in particular to convert LASCO and Mauna Loa spatial resolutions and UVCS spatial and spectral resolutions to those of the METIS instrument.

Table 1: METIS instrumental parameters[1]	
Equivalent focal length	305 mm
Pixel size	15 μm
Detector size	2048×2048 pixels
Spatial resolution (img. channel)	10.14 arcsec/pixel
Spatial resolution (spec. channel)	34 arcsec/pixel
Spectral resolution (H Ly-α channel)	0.54 Å/pixel
Spectral resolution (He II channel)	0.13 Å/pixel
Passband filter width (spec. channel)	80 Å
Coronagraph FOV	1.3°-3.0°
Slit altitudes	1.4°, 1.7°, 2.0°
Slit separation	0.8°

[1]from EID-B (issue 2, rel.2, 03/02/2010)

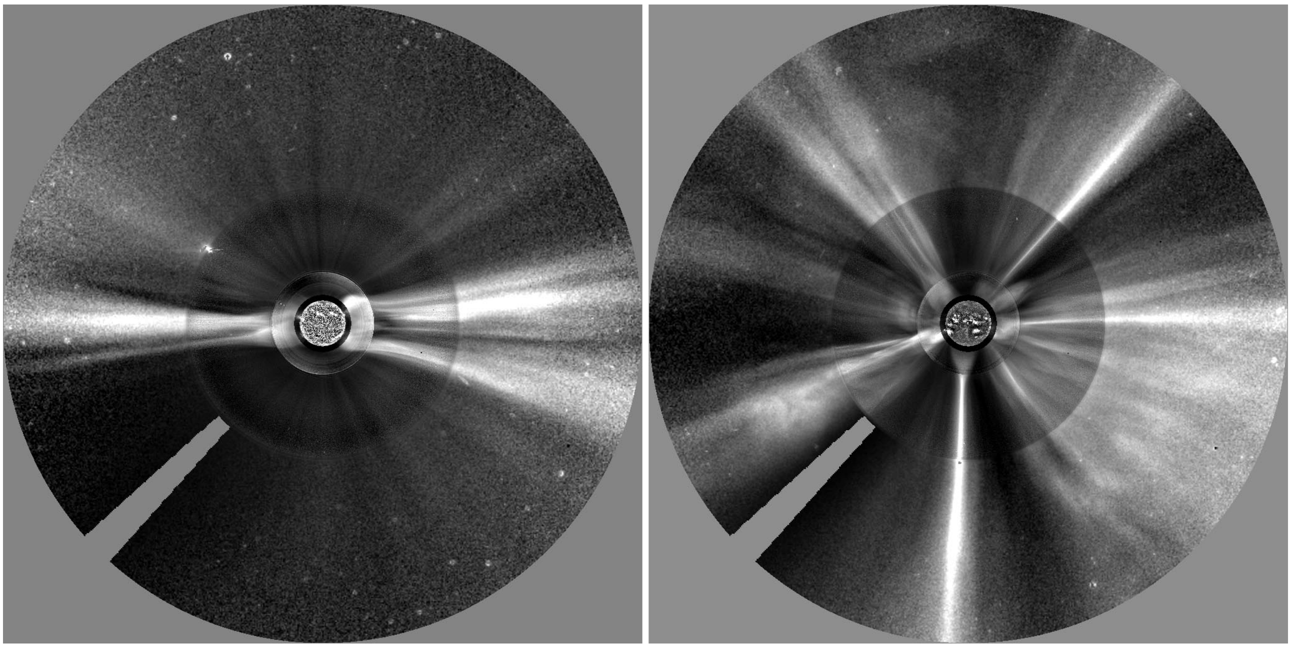

Figure 1: example of input composite MarkIV+LASCO C2+LASCO C3 coronographic white light images provided by the IfA on-line catalog (see text).

2. INPUT IMAGES, INTENSITIES AND SPECTRA

The input white light coronagraphic images have been downloaded from the IfA Catalog of Solar Data Products[1], providing composite MarkIV + LASCO C2 + LASCO C3 images (Fig. 1). These three instruments observe the white light corona with different field of views and different spatial resolutions. IfA catalog provides at least one composite image per day, when data are available from all three instruments at the same time. Composite images provided by the IfA catalog have been already coaligned and each image has a resolution of 1024×1024 pixels; hence, in these images, MarkIV and LASCO C2 spatial resolutions have been downgraded to the LASCO C3 resolution (~56 arcsec/pixel), which is approximately 5 times larger than the METIS resolution (~10 arcsec/pixel). Figure 1 shows an example of composite images representative of the corona white light appearance at the minimum (left) and maximum (right) of solar activity.

Input Lyman-α intensities (phot cm^{-2} s^{-1} sr^{-1}) have been assumed from UVCS data observations. In particular, I assumed the integrated line intensity profiles vs. altitude provided by S. Giordano in the "Counts rate Estimates – METIS Instrument Performance" document (issue 2, rev.2, 11/12/2007). A power law fitting to the profiles provided in this document yields the following analytic expressions for the H Lyman-α line intensity (phot cm^{-2} s^{-1} sr^{-1}) as a function of the heliocentric distance h (see Fig. 2) at the equatorial (I_{eq}) and polar (I_{po}) regions for the minimum and maximum phases of solar activity cycle:

$$I_{eq,\min}(Ly\alpha) = 4.85\times10^{10}\left(\frac{518.56}{h^{11.07}}+\frac{32.17}{h^{5.1}}+\frac{1.29}{h^{2.32}}\right); \quad I_{po,\min}(Ly\alpha) = 2.04\times10^{9}\left(\frac{2155.27}{h^{10.77}}+\frac{128.98}{h^{6.73}}\right)$$

$$I_{eq,\max}(Ly\alpha) = 1.72\times10^{10}\left(\frac{2258.13}{h^{6.807}}+\frac{6.903}{h^{2.197}}\right) \quad ; \quad I_{po,\max}(Ly\alpha) = 2.63\times10^{9}\left(\frac{3194.05}{h^{7.996}}+\frac{262.17}{h^{3.92}}\right)$$

[1] See internet page http://alshamess.ifa.hawaii.edu/prototype/index.php .

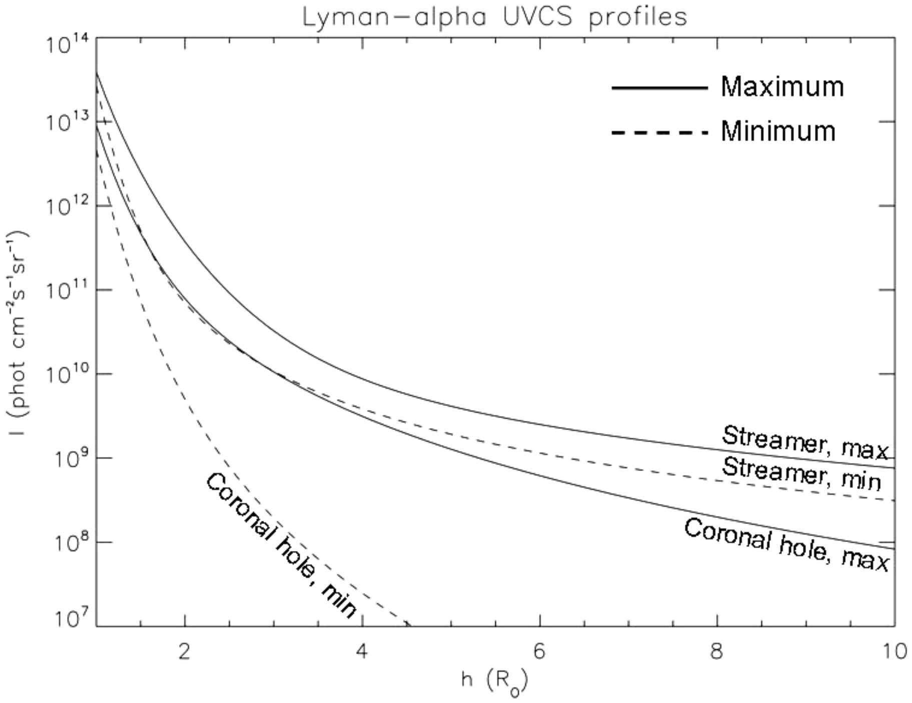

Figure 2: example of input Lyman-α intensity profiles measured by UVCS (see text).

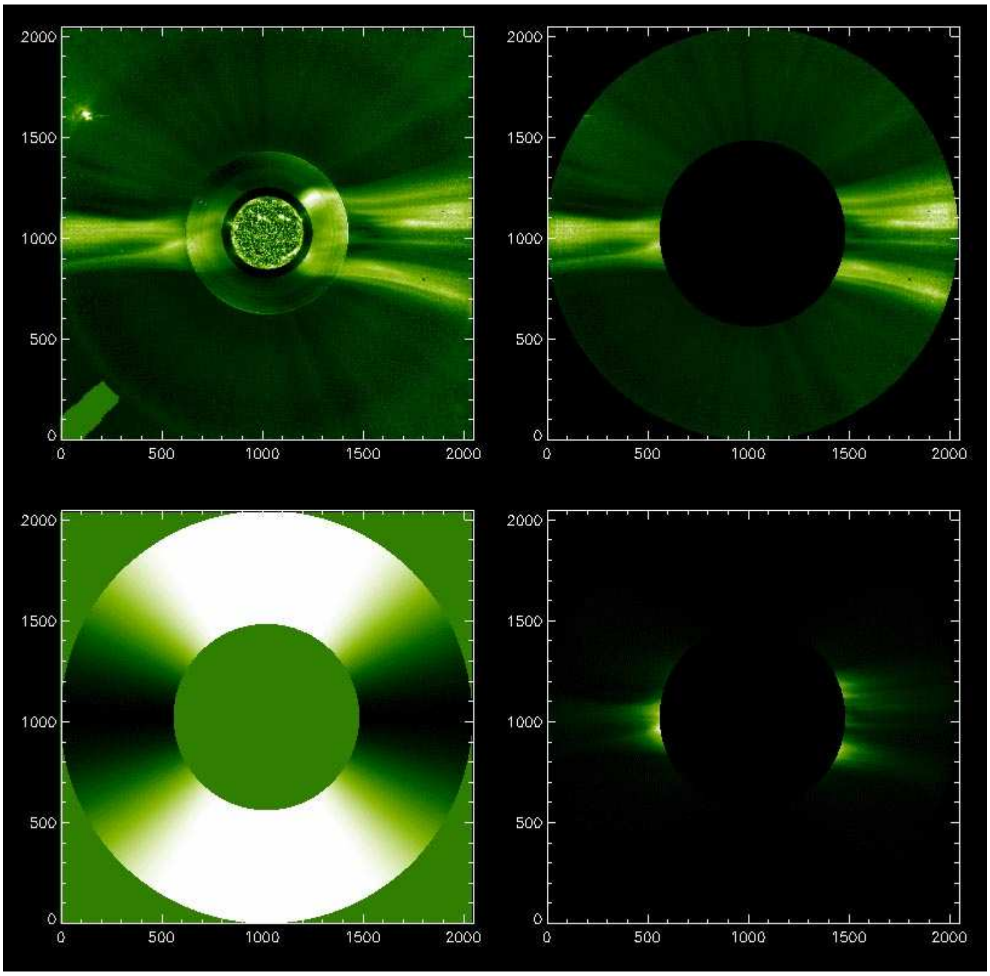

Figure 3: example of successive steps followed to build a 2-D Lyman-α intensity image; this example refers in particular to a spacecraft heliocentric distance of 0.5 AU.

3. BUILDING THE CORONAGRAPHIC IMAGES

The successive steps followed to build a H Lyman-α coronagraphic image are:

1. Convert the composite 1024×1024 white light image to a 2048×2048 image with the correct METIS spatial resolution (km/pixel) expected for the actual heliocentric distance of the Solar Obiter spacecraft (Fig.3, top left);
2. Normalize the white light image to the average radial intensity profile (obtained averaging over 90 radial profiles extracted from the input image, one profile each 4°);
3. Overplot the outer and inner edges of METIS coronagraph field of view (Fig.3, top right);
4. Apply a trigonometric multiplying function f(θ) (where θ is the solar latitude), with $0 \leq f \leq 1$, to scale the 2-D normalized image to the UVCS polar and equatorial Lyman-α intensities (Fig.3, bottom left).

An example of Lyman-α image resulting from the above procedure is shown in Fig.3 (bottom right). In particular, in the resulting image the radial intensity profiles extracted above the pole or at the equator coincides with the UVCS intensity profiles at that latitudes, while at intermediate latitudes the intensities are intermediate between polar and equatorial intensities. The resulting image also mimic the presence of coronal structures: the relative contrast between the streamer structures and nearby coronal hole intensities has been preserved.

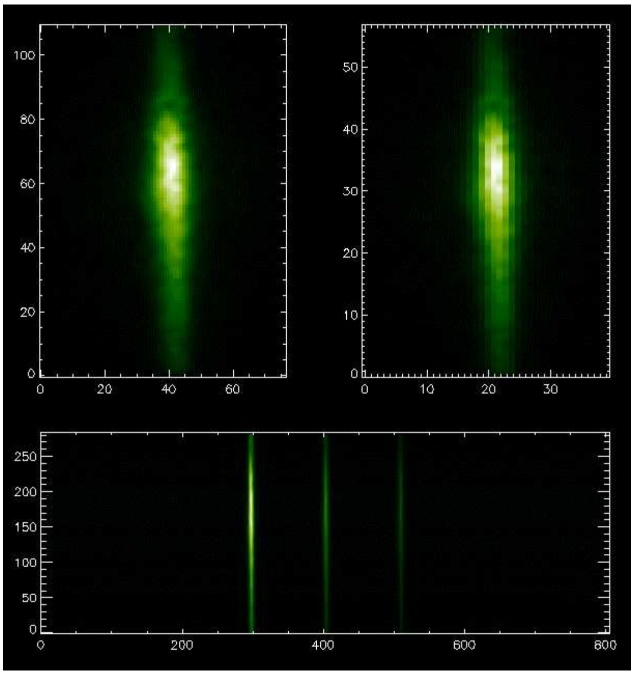

Figure 4: the input UVCS Lyman-α spectra along the slit (top left) and the same spectra adapted to METIS resolutions (top right). These spectra have been used to simulate the total METIS spectrum from the 3 slits.

4. BUILDING THE SPECTRO-SCOPIC IMAGES

The simulated METIS spectrum has been created starting from a Lyman-α spectrum observed by SOHO/UVCS with the Ly-α channel. In particular, in this first attempt I used the spectra acquired by UVCS on December 23, 1996 (file d96.12.23.20_40_59.lya.dat): the reason is that a strong Coronal Mass Ejection (CME) was also observed in this day, hence the same dataset has been used to also simulate the expected spectrum at the CME arrival. In particular, these UVCS observations have been acquired with the slit centered at 1.5 solar radii at a latitude of 55°SE; spectra have been acquired with spectral, spatial and temporal resolutions of 0.1437 Å/pixel, 21 arcsecs/pixel and 300 s/exposure, respectively. The successive steps followed to build a H Lyman-α spectrum as expected from the 3 METIS slits are:

1. Assume the UVCS spectrum acquired at the first exposure (before the CME arrival) as representative of a typical coronal spectrum;
2. Downgrade the spectrum from UVCS (0.1437 Å/pixel, 21 arcsecs/pixel) to METIS (0.54 Å/pixel, 34 arcsecs/pixel) spectral and spatial resolutions;
3. Create 3 spectra for each one of the 3 slits;
4. Create the resulting total spectrum.

For step 3, the intensity observed at each bin has been scaled in order to provide 3 different spectra with an integrated line intensity which, at the slit center, equals the Lyman-α intensity expected (from the above UVCS intensity vs. altitude profiles) on the equator at the actual projected altitude of observation of each slit. Hence, at this first stage, the line intensity decays along the slit is not representative of the real decay expected at the actual altitude of observation; moreover, Lyman-α line widths are assumed to be the same at all altitudes. These two points will be addressed in the next future, in order to provide more reliable simulated spectra.

The spatial extension ΔY (pixels) in the vertical direction Y of the detector region covered by the METIS spectra is simply determined by 0.8×3600/10.14 ~ 284 pixels. The extension ΔX (pixels) in wavelength $\Delta\lambda$ (i.e. in the X direction) of each spectrum produced by the each one of the 3 METIS slits is fixed by the pass-band filter width (see Table 1), i.e. $\Delta\lambda$ = 80Å. Because the first and last slit are separated by 2×0.8° = 1.6°, which corresponds to 1.6×3600/10.14 ~ 568 pixels, while the spectrum extension $\Delta\lambda$ corresponds to 80/0.54 ~ 148 pixels, the total extension ΔX is 716 pixels. Hence the total detector area covered by METIS spectroscopic channel is a rectangle with sixes of 716×284 pixels^2.

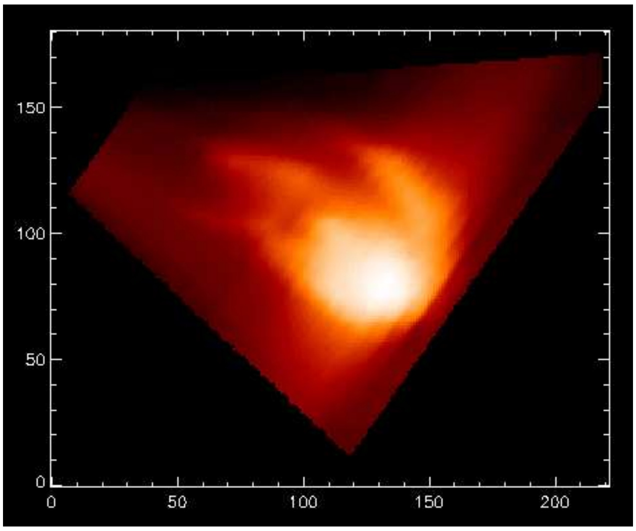

Figure 5: the UVCS Lyman-α CME image built from the spectra observed during the CME occurrence.

The UVCS exposures acquired in the same dataset during the CME arrival have been used to build a Lyman-α CME image. The image (Fig. 5) has been built by assuming that the CME is simply expanding isotropically in the radial direction with the velocity provided by the LASCO-CME catalog (courtesy of S. Giordano). The Lyman-α peak CME intensity has then been scaled, depending on the actual METIS field of view, to the intensity provided by the same power law used for the UVCS Lyman-α streamer intensity at the maximum phase of solar activity.

UVCS spectra acquired during the CME transit have been used not only to produce a simulated Lyman-α CME image, but also to produce a simulated Lyman-α spectrum. To this end, CME spectra from the central (second) METIS slit have been assumed to be equal to UVCS spectra scaled, as mentioned above, with the maximum streamer power law, while peak intensities of simulated spectra from the left (first) and right (third) METIS slits have been scaled by assuming the same CME intensity decrease with altitude as reported by Bemporad et al. (2007, ApJ, 655, 576). In particular, in this work (the only one where the *same* CME has been observed by UVCS at two different altitudes) the authors reported a OVI 1032 Å intensity decrease between 1.6 and 1.9 solar radii by a factor ~2.6.

When METIS will observe spectroscopically a CME the event will not be observed from the imaging channel and vice-versa. In order to show at the same time the CME Lyman-a spectra and image, the latter has been rotated by 90° and placed out of the equatorial plane. The resulting METIS simulated images have been produced by simply adding the simulated spectra to the simulated coronagraphic image (see images in *appendix*).

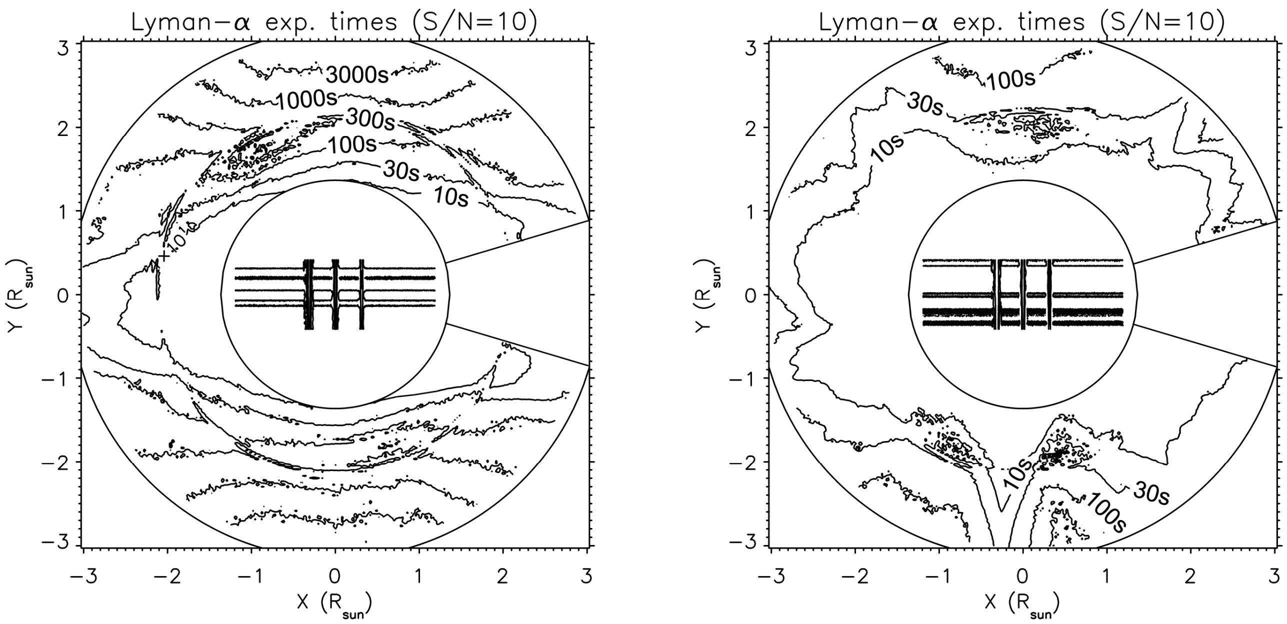

Figure 6: example of computed METIS exposure times required for the Lyman-α channel at the minimum (left) and maximum (right) phases of solar cycle in order to have a signal to noise ratio S/N = 10.

5. ESTIMATE OF REQUIRED EXPOSURE TIMES

The simulated METIS images can be used to estimate the exposure times required at different heliocentric distances of the Solar Orbiter Spacecraft in order to have a fixed signal to noise (*S/N*) ratio. To this end it is necessary to know:

- Vignetting function: is a function $f(\theta)$ only of the angular distance θ from the occulter center. Given $f(\theta)$, a 2D vignetting image V can be computed.
- Mirror reflectivity *M*; Filter transmission *F*; Entrance pupil *R*. Given these quantities, the effective area A_{eff} is $A_{eff} = \left(\pi R^2\right) F M^2 f(\theta) \quad (cm^2)$
- Detector quantum efficiency Q; given all the above quantities and the spectral line integrated radiances I_{line}, the expected counts C_{line} are $C_{line} = I_{line}\, Q\, A_{eff} \quad (cts\ s^{-1} pix^{-1})$
- By assuming a fixed S/N ratio it is possible to derive, given the above quantities, the required exposure times t_{exp} at each altitude.

Required exposure times have been computed by assuming that the noise *N* is due only to the Poissonian statistic, i.e. $N = S^{1/2}$; hence *S/N* = 10 implies *S* = 100 counts. Given a fixed *S/N* ratio and a number of expected counts C_{line} (counts/s), the exposure time t_{exp} (s) required to have this *S/N* ratio for a single pixel is simply $t_{exp} = (S/N)^2 / C_{line}$.

An example of resulting exposure times computed for S/N = 10 when the spacecraft will be at a distance of 0.28 AU is shown in Fig.6 for minimum (left) and maximum (right) of solar activity cycle. In this computation I assumed $f(\theta) \equiv 1$ and (from D. Moses document of 30/11/2009) *M*(Ly-α) = 0.27, *F*(Ly-α) = 0.22 (Al/MgF2), *Q*(Ly-α) = 0.30. Images in Fig.6 show that at solar minimum very long exposure times (up to more than ~ 3000s) will be required over the polar regions in order to have a good S/N ratio, while exposure times of ~ 30s will be sufficient for the equatorial regions; on the contrary, at solar maximum no more than ~ 100s will be required in polar regions. These limits will be more stringent for the spectroscopic channel: in fact, in order to have the same S/N ratio at the peak of the Lyman-a spectral line, by neglecting the background noise, it will be necessary to observe for a time t_{exp}(peak) given by

$$t_{\exp}(peak) = t_{\exp}\frac{\sigma\sqrt{2\pi}}{r}$$

where r = 0.54 Å/pixel is the Lyman-α channel spectral resolution and σ is in Å. For instance, by assuming a FWHM = 1 Å, hence σ ~ 0.42 Å, it turns out that the exposure times required on the METIS spectroscopic channel in order to have at the line peak the same *S/N* ratio than what required in the imaging channel are a factor ~ 1.9 ≈ 2 larger.

6. APPENDIX

Images given in the following appendix are:

1. Solar maximum corona observed by METIS with Solar Orbiter at 0.28 AU
2. Solar maximum corona observed by METIS with Solar Orbiter at 0.50 AU
3. Solar maximum corona observed by METIS with Solar Orbiter at 0.72 AU
4. Solar minimum corona observed by METIS with Solar Orbiter at 0.28 AU
5. Solar minimum corona observed by METIS with Solar Orbiter at 0.50 AU
6. Solar minimum corona observed by METIS with Solar Orbiter at 0.72 AU
7. Solar maximum corona + CME observed by METIS with Solar Orbiter at 0.28 AU
8. Solar maximum corona + CME observed by METIS with Solar Orbiter at 0.72 AU

1)

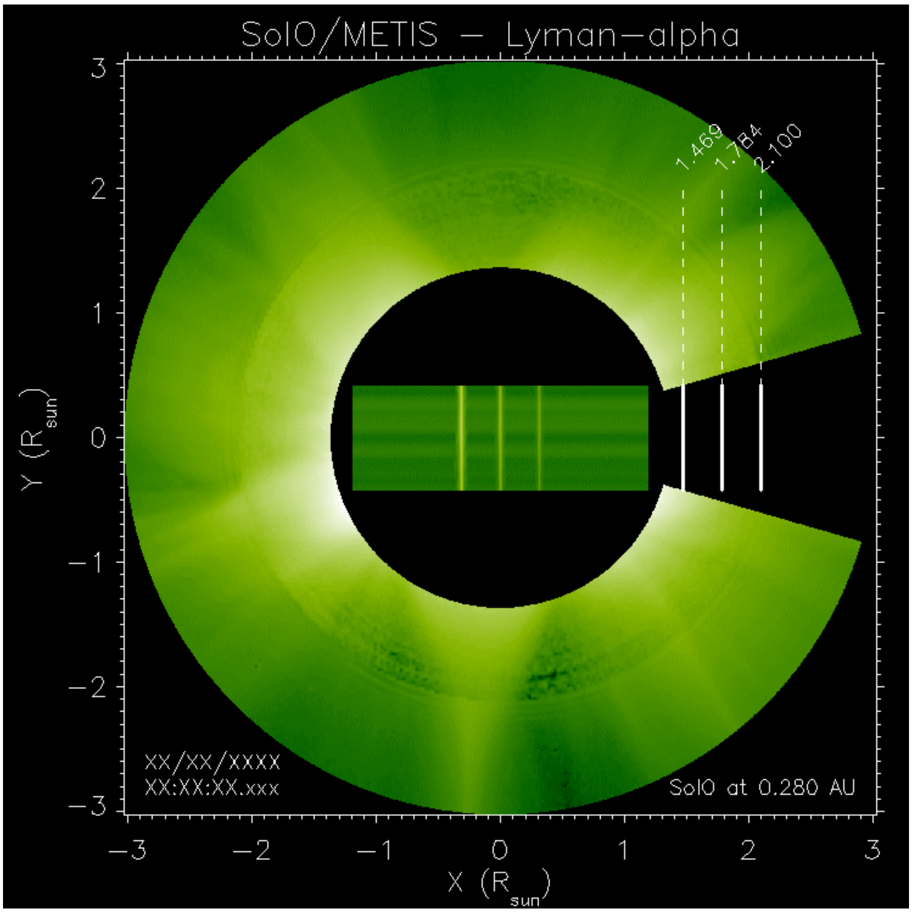
SolO/METIS – Lyman–alpha
1.469
1.784
2.100
XX/XX/XXXX
XX:XX:XX.xxx
SolO at 0.280 AU
X (R_{sun})
Y (R_{sun})

2)

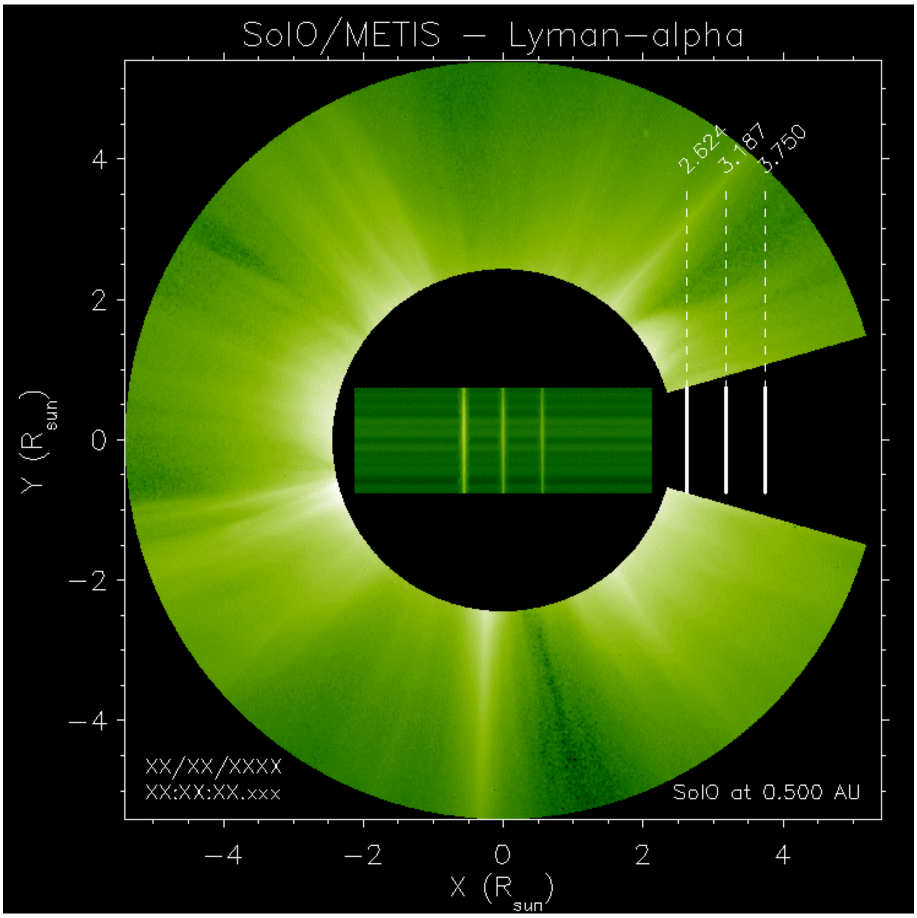
SolO/METIS – Lyman–alpha
2.624
3.187
3.750
XX/XX/XXXX
XX:XX:XX.xxx
SolO at 0.500 AU
X (R_{sun})
Y (R_{sun})

3)

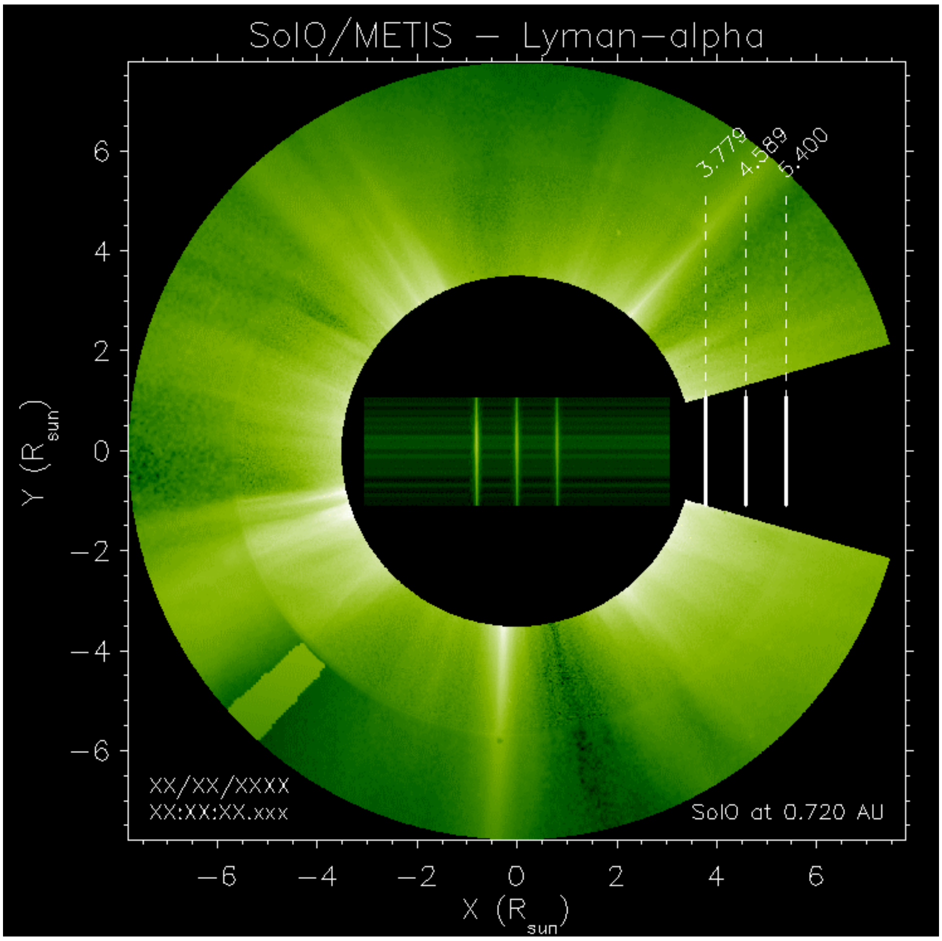
SolO/METIS – Lyman–alpha
3.779
4.589
5.400
XX/XX/XXXX
XX:XX:XX.xxx
SolO at 0.720 AU
Y (R_{sun})
X (R_{sun})

4)

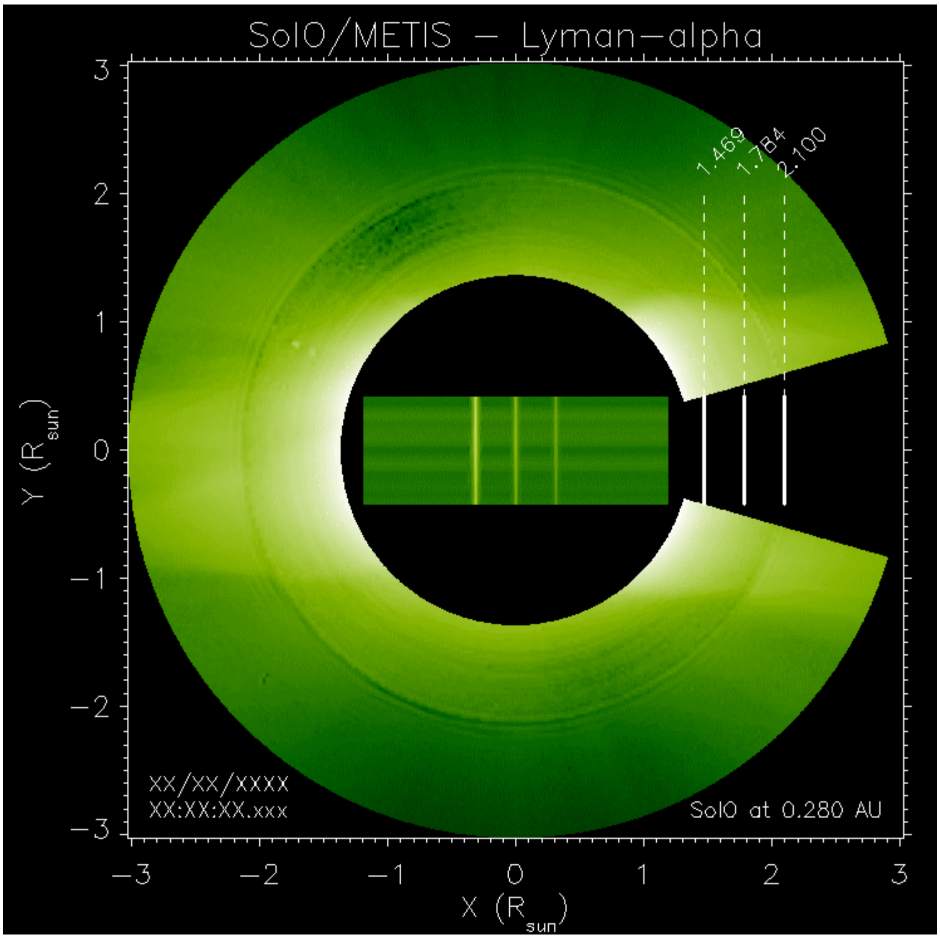
SolO/METIS – Lyman–alpha
1.469
1.784
2.100
XX/XX/XXXX
XX:XX:XX.xxx
SolO at 0.280 AU
Y (R_{sun})
X (R_{sun})

5)

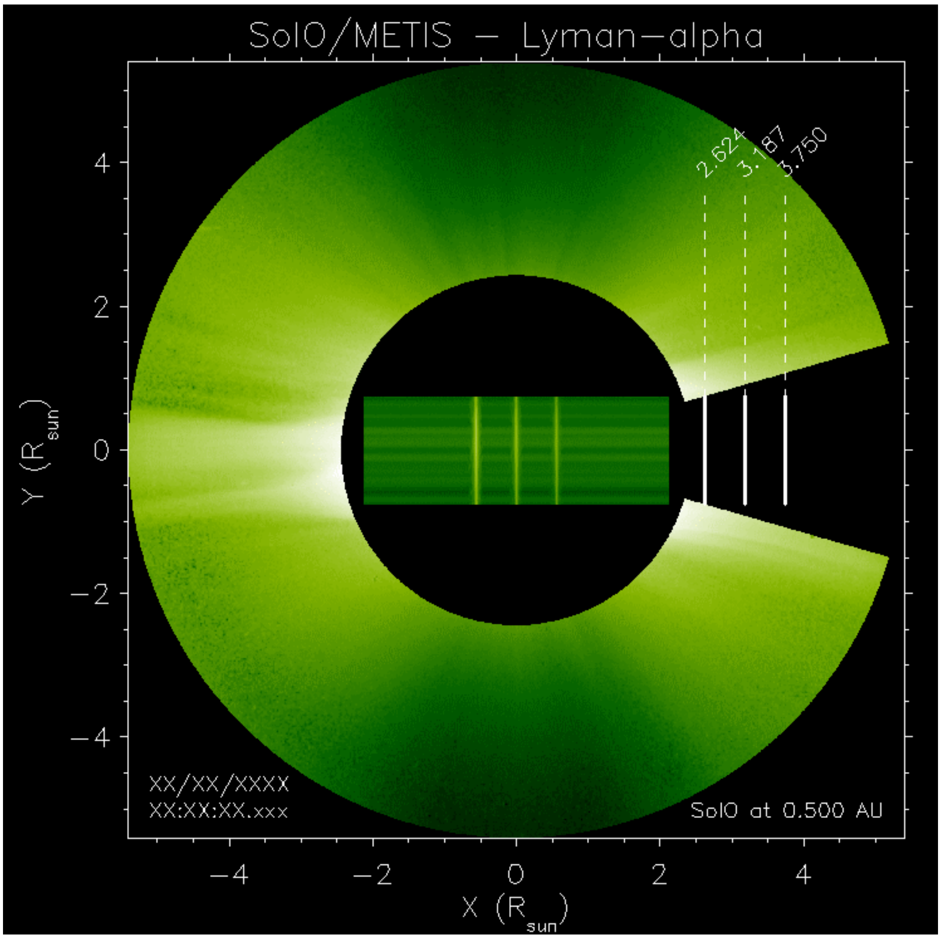
SolO/METIS – Lyman–alpha
2.624
3.187
3.750
Y (R$_{sun}$)
X (R$_{sun}$)
XX/XX/XXXX
XX:XX:XX.xxx
SolO at 0.500 AU

6)

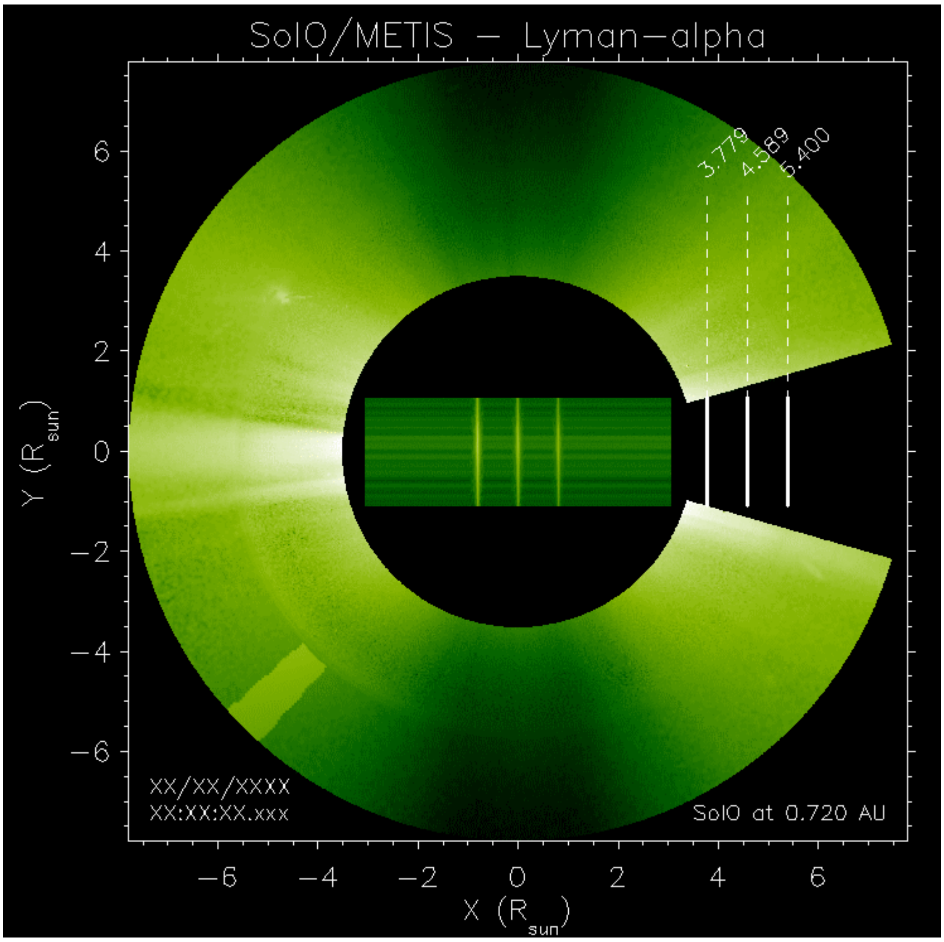
SolO/METIS – Lyman–alpha
3.779
4.589
5.400
Y (R$_{sun}$)
X (R$_{sun}$)
XX/XX/XXXX
XX:XX:XX.xxx
SolO at 0.720 AU

7)

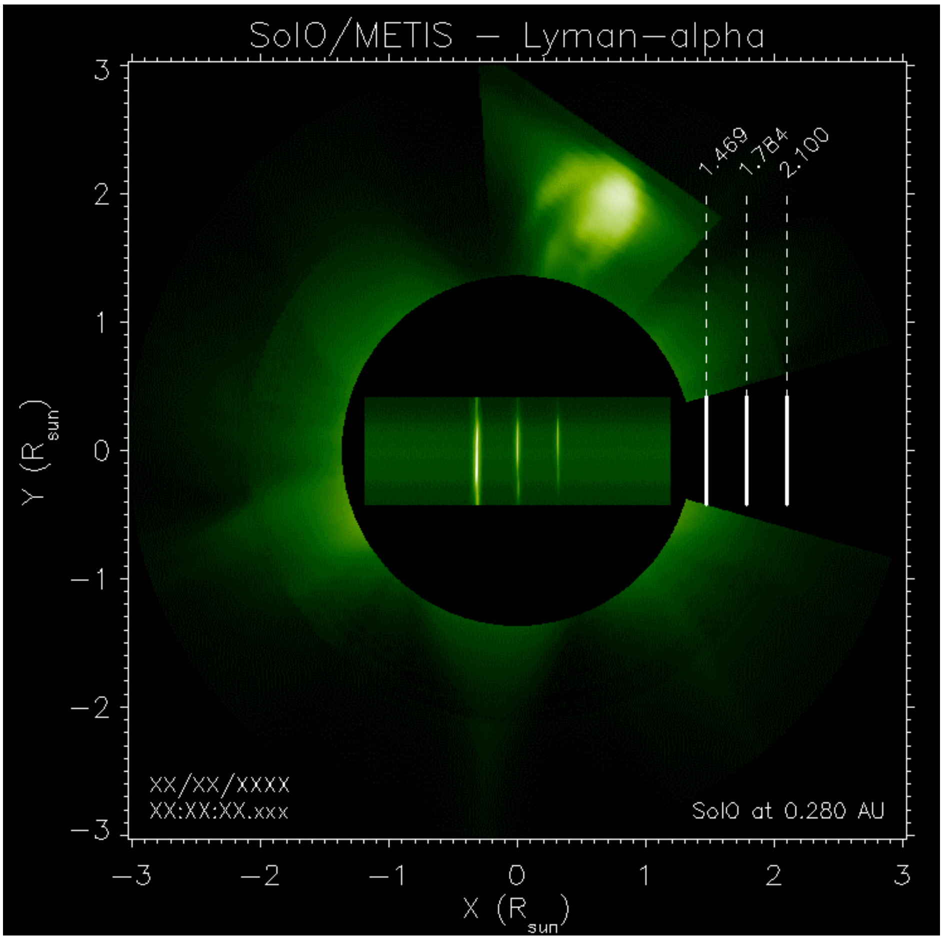
SolO/METIS – Lyman–alpha
1.469
1.784
2.100
XX/XX/XXXX
XX:XX:XX.xxx
SolO at 0.280 AU
Y (R$_{sun}$)
X (R$_{sun}$)

8)

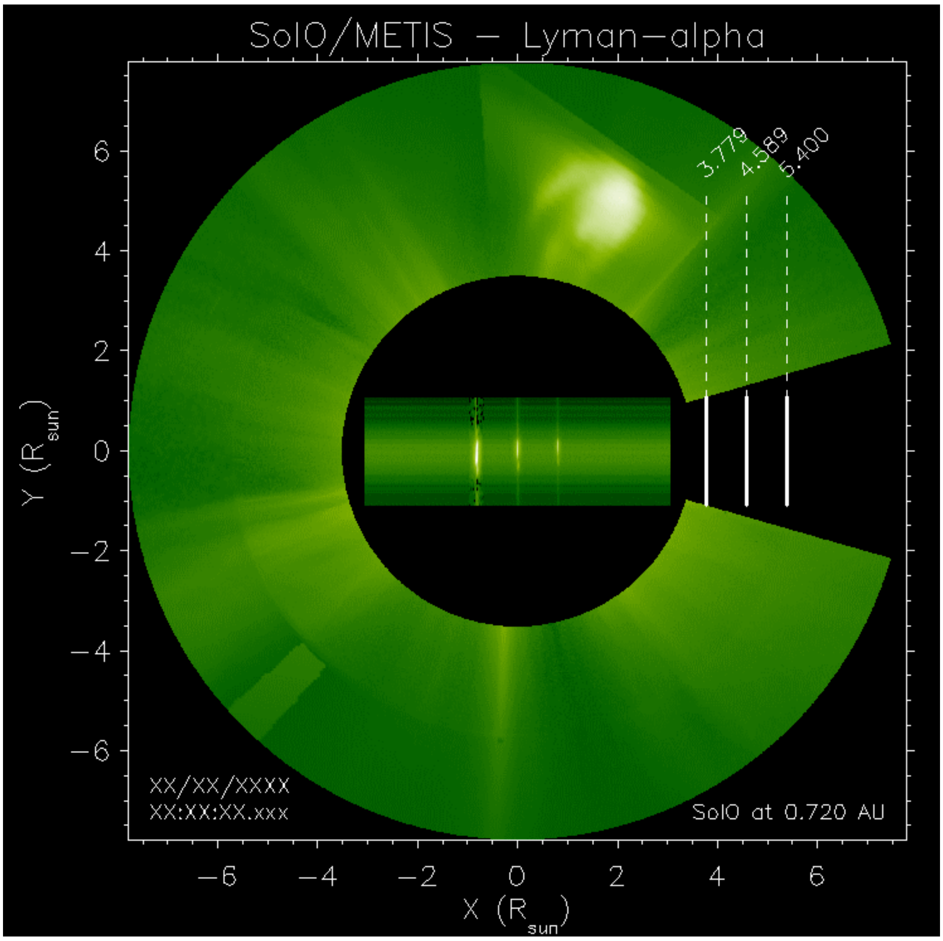
SolO/METIS – Lyman–alpha
3.779
4.589
5.400
XX/XX/XXXX
XX:XX:XX.xxx
SolO at 0.720 AU
Y (R$_{sun}$)
X (R$_{sun}$)